

3D FRICTIONAL CONTACT AND IMPACT MULTIBODY DYNAMICS: A COMPARISON OF ALGORITHMS SUITABLE FOR REAL-TIME APPLICATIONS

M. Renouf^{†*}, V. Acary* and G. Dumont[†]

[†] Siames Project, IRISA/ INRIA Rennes
Campus Universitaire de Beaulieu Avenue du Général Leclerc 35042 RENNES Cedex - France
e-mail: Georges.Dumont@irisa.fr, Mathieu.Renouf@irisa.fr

^{*}Bipop Project, INRIA Rhône-Alpes
ZIRST Montbonnot, 655, avenue de l'Europe, 38334 Saint ISMIER, France
e-mail: Vincent.Acary@inrialpes.fr

Keywords: 3D frictionless/frictional unilateral contact, real-time, time-stepping scheme, direct and iterative methods, linear and nonlinear complementarity problems.

Abstract. *During the last decade Virtual Reality has benefited of numerous works dedicated to the modeling and the simulation of multibody systems. Even if a large set of methods are already used by the community of computer graphics and virtual reality, some progresses need still to be made to bridge the gap between accurate mechanical simulation and efficient simulations in real-time of realistic systems. Particularly, the problem of the three dimensional frictional contact with impacts is a key point for the applications with haptic feedback. The work aims at adapting the outstanding methods in computational mechanics to the real-time constraints induced by Virtual Reality. For efficiency reasons, our work is based on the Non Smooth Contact Dynamics (NSCD) framework introduced by Moreau (1988). Two major advantages of the method can be exhibited for the real-time context: the method uses a time-stepping numerical scheme without explicit event-handling procedure and an unilateral contact impact formulation associated with the 3D Coulomb's friction law. In the present paper, we use and compare different iterative algorithms (Non Smooth Gauss-Seidel, projected conjugate gradient, the PATH solver) for complementarity problems with a direct one (Lemke). The efficiency of the methods is compared in terms of complexity, of quality ratio between visual feed-back of solution and convergence criterion and of CPU time keeping in mind the real-time constraint.*

1 Introduction

Fast simulations of multibody systems appear as a recurrent theme in Computer Graphics [6, 16], in Robotics [23] and in Computational Mechanics [8]. Since more than fifteen years, the Computer Graphics community has developed and optimized several numerical methods for 3D simulations of multibody systems. To ensure the realism of a 3D scene, the simulation of the motion and of the interaction between objects must respect the fundamental principles of Mechanics and Thermodynamics and at least, the basic behavior required by the Physics. For the virtual reality, the challenge is to reach this goal together with the real-time constraint.

To face this problem one solution is to adapt the methods of computational mechanics for the real-time simulation of multibody systems. The work of the Computational Mechanics community focuses on an accurate description of interaction through a theoretical, experimental and numerical framework. In this context, the real-time constraint can hardly be preserved due to the complexity of models which leads to heavy computations. The non smooth mechanics approach, together with adapted numerical methods based on a time-stepping scheme and some iterative solvers can be however an alternative to perform real-time mechanical simulations of multibody systems.

Outline of the paper The purpose of this paper is to present a comparison between several algorithms in view of real-time simulations based on the *Non Smooth Contact Dynamic* (NSCD) framework (Moreau [30, 31, 32] and Jean [19]). In Sec. 2 we give a brief overview of the related works in the Computer Graphics, Virtual Reality and Computational Mechanics communities. We expose, in Sec. 3, the equations and the basic equations within the NSCD formalism. In Sec. 4, the numerical scheme for the time integration is presented. Various formulations of the time-discretized multibody dynamics are provided in Sec. 5 in order to prepare the introduction of different numerical solvers in Sec. 6. Finally, the results on different kind of simulations are resumed in Sec. 8 and Sec. 9 concludes the paper.

2 Related Works

2.1 Computer Graphics and Virtual reality community

Computer graphics community In the computer graphics community, simulations have to reach at least one goal: a perfect visual feedback. Usually, the question of the real-time constraints is pushed into the background. Among the first attempt to simulate the mechanics of rigid bodies with contact, we can cite the work of Hahn [17] and Moore and Wilhems [29]. They used analytical methods to compute forces in colliding rigid body systems. To prevent violation between bodies during a resting contact, Hahn [17] modeled the contact as a series of collisions. Moore and Wilhems [29] used a penalty method (compliant contacts) to prevent the penetration using the admitted overlapping between the bodies in contact.

Baraff [6] was the first to propose a method to calculate dynamically the contact forces (constraints-based method). First of all, he dealt with two-dimensional non-penetrating and non-colliding polygonal objects and used an analytical method to solve the contact problem. It will be formulated as a linear complementarity problem (LCP) and resolved using fast pivoting methods Baraff [7] without the use of numerical optimization software currently used to solve linear programming (LP) or quadratic programming problem (QP) and with a separate treatment of contact and collisions in an event-driven integrator.

Mirtich and Canny [27] proposed an impulse-based approach to deal with rigid bodies simulations. They checked for the moment of contact and did not deal with concurrent impacts, which

can lead to slow time of simulation when virtual systems are compact assemblies. Moreover the resting contact is treated by using a collision threshold and by applying a micro-collision model to the relative velocity between bodies in contact.

A position-based approach is proposed by Milenkovic [25] to simulate piles of polygonal and spherical objects using a potential energy depending only on the position of the bodies. His approach deals with non-rotating bodies and does not take into account the velocity. With Schmidl [26], they adjusted the predicted position of bodies using optimization-based methods. Stacking of bodies (less than one hundred) does not always display a realistic behavior. Improvements based on a “freezing” technique [41] allow to deal with packing of 1 000 cubes. However the mechanical properties are lost and the simulation does not respect the real-time constraint. Guendelman et al [16] considered new algorithms to simulate large assemblies of convex and non convex rigid bodies. They dealt with shock propagation method (and not simultaneous) to treat contact. With their time integration scheme they update twice the velocity related to a separation of contact and collision resolution in the equation of motion. The results are visually accurate but the graduation of restitution to improve the accuracy of their propagation model can be discussed.

Virtual Reality community In the context of Virtual Reality, the visual feedback is one of the goal to reach, but one need also to ensure a good modeling of forces and motions for instance, for an haptic feedback. The hard constraint is to ensure these properties in real-time contrary to the usual cases in Computer Graphics.

Schömer and co-workers [38, 9] proposed a constraint-based approach where equations of motion are described by a non-linear complementarity problem (NCP) solved using a Lemke algorithm. The efficiency of the method on large systems is not brought up. More recently Hasegawa et al [18] consider the shape of the surface intersection instead of the overlap. Although these approaches are fast, they need small time steps to secure the stability of the numerical scheme and even smaller to capture all binary collisions in large collections of rigid bodies.

2.2 Computational Mechanics

We leave the works on the quasi-static contact mechanics between deformable bodies out. Indeed, such approaches are not well suited for the dynamics with contact, friction and impact. In the computational mechanics community, we found the two dualities between compliant/unilateral model and event-driven/time-stepping scheme. In the context of granular materials, where large collections of bodies are encountered, Cundall [11] was the first to propose a numerical tools based on a Euler scheme and where contacts are governed by a compliant model. With a definitely different approach, Moreau [30] and Jean [20, 19] present a treatment of rigid bodies with unilateral contact, Coulomb’s dry friction and impact in the framework of the nonsmooth mechanics and convex analysis. This framework yields a time-stepping scheme (without explicit event-handling) where velocity and impulses are the primary variables. The scheme is a very efficient numerical tool on a great number of applications that are well-known for theirs difficulties. Among them, we can cite recent works on masonry structures [2, 4], granular materials with polygonal et polyhedral shapes [40]. Although in all previous works the real-time constraint not is fulfilled (and it is not the purpose), the numerical efficiency is critical justifying studies and improvements proposed by Renouf et al [36]. Still in a nonsmooth framework, Pfeiffer and Glocker [33] or Stewart and Trinkle [42] designed an event-driven algorithm as time integration scheme and proposed a general formulation of the dynamics at

the acceleration-force level. In [1], a similar work is done where the numerical tools of the Moreau's school are used.

2.3 Motivations

Most of the algorithms proposed by the Computer Graphics community are based on an event-driven approach. In this context, the constrained based approach of Baraff [7] and the impulse based approach of Mirtich [27] are widespread and have proved their efficiencies. Major drawbacks of these approaches remain the treatment of accumulation of events (Zeno-behavior) and a large number of bodies in closed contact. A first attempt to unify this has been done in [16] but the collision case with impulse and the contact case with forces are separated. Nevertheless, the real-time constraint has not been taken into account.

As an alternative to the previous drawbacks, we have chosen to adapt tools of computational mechanics for the real-time simulation of multibody systems. As underlined in the introduction, our work is based on the NSCD framework. The time-stepping scheme is not handicapped by the change of contact status during the simulation. One of the important point is to have a unified treatment of collisions as well as potential, sticking or sliding contacts. It is not necessary to determine the interval of time for which the change of status occurs. Thus each time-step depends only on the geometry, the boundary conditions and the possible nonlinear behavior of the smooth dynamics. Consequently, the time step can be constant and large enough to ensure fast computations. The theoretical results on the convergence of such schemes proposed by [28, 24] is also a strong point for this time-integration scheme. Moreover the general character of such a formulation allows to use a large panel of numerical methods for the time-discretized problem.

Our computational mechanical software platform is embedded in OpenMASK, a virtual reality open-source middle-ware (<http://www.OpenMASK.org>) and simulations have been performed on an Opteron 242 with a 2 GHz processor.

3 Multicontact Rigid Body systems

3.1 Parametrization

Let $\mathbf{q} = (q_1, \dots, q_N)$ be $\in \mathbb{R}^N$ the generalized coordinates vector of a collection of n_b rigid bodies, with $N = 6n_b$. For the sake of simplicity, we assume that the eventually bilateral liaisons imposed to the system have been taken into account by reducing the size of \mathbf{q} . The unilateral constraints of non penetration are expressed by the following set of inequalities:

$$f_\alpha(t, \mathbf{q}) \geq 0, \quad \alpha \in \{1, \dots, n_c\}. \quad (1)$$

Each function f_α depends both on the configuration parameter \mathbf{q} and the time t . This double dependency involves a geometric constraint between bodies, which can not overlap one each other (\mathbf{q} dependency) and some external obstacles moving in time (*time* dependency). When the equality occurs ($f_\alpha = 0$) it corresponds to the existence of a closed contact in the system (the gap between bodies is reduced to zero). The result of the interaction of the antagonist body \mathcal{B}_a on the candidate one \mathcal{B}_c can be described by a simple force \mathbf{r}_α acting at a contact point I_α . At this same point, we can define a local frame \mathcal{F}_α composed of three vectors: a normal one, \mathbf{n}_α , pointing from \mathcal{B}_a to \mathcal{B}_c and two tangential ones \mathbf{s}_α and \mathbf{t}_α , which define the tangential space. By convention $\mathbf{s}_\alpha \times \mathbf{t}_\alpha = \mathbf{n}_\alpha$. We denote g_α the gap between bodies along the normal direction. This value is negative when the bodies overlap. The local forces $\mathbf{r}_\alpha \in \mathbb{R}^3$, expressed in the local

frame are related to the global one $\mathbf{R}_\alpha \in \mathbb{R}^N$ by a linear relation:

$$\mathbf{R}_\alpha = \mathbb{H}_\alpha(\mathbf{q}) \mathbf{r}_\alpha, \quad (2)$$

where $\mathbb{H}_\alpha(\mathbf{q}) : \mathbb{R}^N \rightarrow \mathbb{R}^{N \times 3}$ is a mapping, which contains the local information about contactors. Each component \mathbf{R}_α can be understood as the contribution of contact α to the global forces and can be decomposed into $n_b - 2$ null vectors ($\in \mathbb{R}^6$) and two vectors $\mathbf{R}_{\alpha,c}$ and $\mathbf{R}_{\alpha,a}$ corresponding respectively to the torque of the candidate body and the antagonist one. The construction of the global contact forces vector is denoted formally by

$$\mathbf{R} = \sum_{\alpha} \mathbf{R}_\alpha. \quad (3)$$

In the same way, the velocity of the bodies can be expressed in the local frame \mathcal{F}_α . We define the relative velocity \mathbf{u}_α at the contact point I_α between \mathcal{B}_a and \mathcal{B}_c by the relation,

$$\mathbf{u}_\alpha = \mathbb{H}_\alpha^*(\mathbf{q}) \dot{\mathbf{q}}, \quad (4)$$

where \mathbb{H}^* is the transpose of \mathbb{H} . The relative velocity \mathbf{u}_α is decomposed in a normal part represented by $u_{\alpha,n}$ and a tangential one $\mathbf{u}_{\alpha,T} = (u_{\alpha,s}, u_{\alpha,t})$. Note that the derivative of gap function $t \rightarrow g_\alpha(t)$ is equal to $\mathbf{u}_\alpha \cdot \mathbf{n}_\alpha$. For the sequel, we define the mapping $\mathbb{H}(\mathbf{q}) : \mathbb{R}^N \rightarrow \mathbb{R}^{N \times 3n_c}$ as the aggregation of the matrices \mathbb{H}_α .

3.2 Equation of Dynamics

When some smooth motion describes the evolution of the system, the dynamical equation is

$$\mathbb{M}\ddot{\mathbf{q}} = \mathbf{F}(t, \mathbf{q}, \dot{\mathbf{q}}) + \sum_{\alpha} \mathbf{R}_\alpha, \quad (5)$$

where \mathbb{M} is the inertia matrix and $\mathbf{F}(t, \mathbf{q}, \dot{\mathbf{q}})$ the internal and external forces. In multicontact systems, shocks are expected. The velocity may have jumps and the acceleration can not be defined as the usual second derivative of q . Consequently equation (5) must be reformulated in terms of a measure differential equation,

$$\mathbb{M}d\dot{\mathbf{q}} = \mathbf{F}(t, \mathbf{q}, \dot{\mathbf{q}})dt + d\mathbf{R}, \quad (6)$$

where dt is the Lebesgue measure on \mathbb{R} , $d\dot{\mathbf{q}}$ is a differential measure representing the acceleration measure and $d\mathbf{R}$ is a non-negative real measure, which can be decomposed by a standard measure decomposition:

$$d\mathbf{R} = \mathbf{F}_R dt + \mathbf{J}_R. \quad (7)$$

The continuous function \mathbf{F}_R is the usual contact force when the motion is sufficiently smooth and the measure \mathbf{J}_R is the singular part of the measure. This singular part may be composed of a set of Dirac measures which represent jumps in the velocity function due to impacts.

3.3 Frictional contact laws

To describe the motion of our system, some informations are still missing. Additional informations about contact forces must be added to determine the value of each component \mathbf{R}_α . These quantities are essential to complete equation (6) and to describe the motion of our system.

3.3.1 The Signorini Condition

The impenetrability of contact evoked previously means that the body candidates for contact must avoid crossing the boundaries of antagonist bodies. We consider also that the contacting bodies are not attracting each other i.e. the normal component of the reaction force is always positive or equal to zero when the contact vanishes. This contact behavior leads to the well-known *Signorini Condition*:

$$g \geq 0 \quad r_n \geq 0 \quad g.r_n = 0. \quad (8)$$

The complementarity condition can also be expressed in terms of the following inclusion:

$$-r_n \in N_{\mathbb{R}_+}(g) = \partial\Psi_{\mathbb{R}_+}(g), \quad (9)$$

where $N_K(\cdot) = \partial\Psi_K(\cdot)$ is the normal cone to a convex set K , ∂f is the sub-differential of a function f and Ψ_K is the indicatrix function of K . All of this notions are defined in the sense of Convex Analysis [37].

Following the work of Moreau [30], we propose to use a velocity-based formulation, which is well-suited for the numerical purpose:

$$-r_n \in \partial\Psi_{T_{\mathbb{R}_+}(g)}(u_n), \quad (10)$$

where $T_K(\cdot)$ is the tangent cone to K . This inclusion in terms of velocity may be reformulated as the following so-called *velocity Signorini condition*:

$$\text{if } g \leq 0 \text{ then} \quad u_n \geq 0, \quad r_n \geq 0, \quad u_n.r_n = 0. \quad (11)$$

The fact that $\partial\Psi_{T_{\mathbb{R}_+}(g)}(u_n) \subset N_{\mathbb{R}_+}(g)$ and $\dot{g} = u_n$ yields to the Viability Lemma proved in [32] which ensures that (11) implies that the Signorini condition (8) are respected.

3.3.2 The Coulomb's friction law

The dry frictional law is the Coulomb's one for which the basic features are: the friction force lies in the Coulomb's cone ($\|\mathbf{r}_t\| \leq \mu r_n$, μ friction coefficient), and if the sliding relative velocity is not equal to zero, its direction is opposed to the friction force and its modulus is given by $\|\mathbf{r}_t\| = \mu r_n$. We can summarize the previous explanations by the following relation:

$$\begin{cases} \text{if } \|\mathbf{u}_t\| = 0, & \|\mathbf{r}_t\| \leq \mu r_n \\ \text{if } \|\mathbf{u}_t\| \neq 0, & \|\mathbf{r}_t\| = \mu r_n, \mathbf{u}_t = -\kappa \mathbf{r}_t, \kappa \geq 0 \end{cases} \quad (12)$$

The Coulomb's friction law can be also expressed as the inclusion:

$$-\mathbf{u}_t \in N_{C(\mu r_n)}(\mathbf{r}_t), \quad (13)$$

where the convex set $C(\mu r_n)$ is the section of the friction cone. Usually, for an isotropic friction law, the section is a disk of radius μr_n ,

$$C(\mu r_n) = \{\lambda_t, \sigma_C(\lambda_t) = \mu r_n - \|\lambda_t\| \geq 0\}. \quad (14)$$

For some numerical reasons [38, 26] or for a particular frictional behavior, the friction cone may be defined by a pyramid and the section $C(\mu r_n)$ is then a polytope. We will see in the next section the consequence of this facetization of the friction cone on the type of numerical problem that we can state.

3.3.3 A generalized Newton impact law

For rigid bodies, the *velocity Signorini condition* is equivalent to a perfectly plastic impact law. If a ball falls on a horizontal plan, it does not bounce off. To model bounces, an impact law is needed. We choose the Moreau impact law, which is an extension of the classical Newton impact law ($u_n^+ = -e_n u_n^-$) to multicontact systems (e.g. [31]):

$$-r_n \in \partial \Psi_{T_{\mathbb{R}_+}(g)}(u_n^+ + e_n u_n^-), \quad (15)$$

which is equivalent to

$$\text{if } g \leq 0 \text{ then } \quad u_n^+ + e_n u_n^- \geq 0, \quad r_n \geq 0, \quad (u_n^+ + e_n u_n^-).r_n = 0. \quad (16)$$

In spite of the fact that this shock law can not represent all shock phenomena, particularly, concurrent multiple impacts, see [3], it provides us with very satisfactory results for sphere packing and virtual masonry where the propagation of impacts is not the crucial behavior.

3.3.4 Summary

In the following the frictionless or frictional contact law given by (12) and (15) for each couple $(\mathbf{u}_\alpha, \mathbf{r}_\alpha)$ will be denoted by the following formula:

$$\text{law}_\alpha[\mathbf{u}_\alpha, \mathbf{r}_\alpha] = .\text{true}. \quad (17)$$

4 Numerical scheme for the time integration

4.1 Discretization of the dynamics

One of the most interesting features of the time-stepping integration scheme is included in the fact it does not have to handle explicitly the contact events, contrary to the usual event-driven scheme. When we proceed to a time discretization on intervals $]t_i, t_{i+1}]$ of length h , our contact problem is solved over the interval in terms of measures of this interval and not in a point wise way. To achieve this property, the equation (6) is integrated on each subdivision, which leads to

$$\begin{cases} \mathbb{M}(\dot{\mathbf{q}}_{i+1} - \dot{\mathbf{q}}_i) = \int_{t_i}^{t_{i+1}} \mathbf{F}(t, \mathbf{q}, \dot{\mathbf{q}}) dt + \mathbf{R}_{i+1} \\ \mathbf{q}_{i+1} = \mathbf{q}_i + \int_{t_i}^{t_{i+1}} \dot{\mathbf{q}}(t) dt \end{cases}, \quad (18)$$

where the variable $\dot{\mathbf{q}}_{i+1}$ stands for the approximation of the right limit of the velocity at the time t_{i+1} , i.e. $\dot{\mathbf{q}}(t_{i+1}^+)$, and $\mathbf{q}_{i+1} \approx \mathbf{q}(t_{i+1})$. For the contact measure $d\mathbf{R}$, we approximate the measure of the time interval $]t_i, t_{i+1}]$ by $d\mathbf{R}$ denoted by

$$d\mathbf{R}(]t_i, t_{i+1}]) = \int_{]t_i, t_{i+1}]} d\mathbf{R} \triangleq \mathbf{R}_{i+1}, \quad (19)$$

To approximate the two integrals of the system (18), we use a θ -method, which is a first-order scheme using only the configuration parameter and its first derivative. The stability condition

of the scheme implies that θ to remains between $1/2$ and 1 . This approximation leads to the following formula,

$$\begin{cases} \int_i^{t_{i+1}} \mathbf{F}(t, \mathbf{q}, \dot{\mathbf{q}}) ds = h\theta \mathbf{F}(t_{i+1}, \mathbf{q}_{i+1}, \dot{\mathbf{q}}_{i+1}) + h(1 - \theta) \mathbf{F}(t_i, \mathbf{q}_i, \dot{\mathbf{q}}_i) \\ \mathbf{q}_{i+1} = \mathbf{q}_i + h\theta \dot{\mathbf{q}}_{i+1} + h(1 - \theta) \dot{\mathbf{q}}_i \end{cases} \quad (20)$$

For the simplicity sake, we will consider in the sequel that internal and external forces are given by a function of time $F(t)$. In the more general case, a linearizing procedure (Newton scheme) allows us to obtain the same set of discretized equations [19].

The first equation in (18) can be rewritten as

$$\dot{\mathbf{q}}_{i+1} = \dot{\mathbf{q}}_{i,free} + (\mathbb{M}^{-1}) \mathbf{R}_{i+1} \quad (21)$$

with

$$\dot{\mathbf{q}}_{i,free} = \dot{\mathbf{q}}_i + \mathbb{M}^{-1} h(\theta \mathbf{F}_{i+1} + (1 - \theta) \mathbf{F}_i).$$

The θ -method is an implicit scheme, identical to the Backward Euler's one when $\theta = 1$.

4.2 Discretization of the contact law

To complete the discrete form of the dynamical equation, a discretization of the frictional contact law must be performed. We use the formulation proposed by [19], which gives for the velocity *Signorini condition with restitution* (15):

$$-r_{n,i+1} \in \partial \Psi_{T_{\mathbb{R}_+}(\tilde{g}_{i+1})}(u_{n,i+1} + e_n u_{n,i}), \quad (22)$$

where $\tilde{g}_{i+1} = g_i + h u_{n,i}$ is a prediction of the gap. For the Coulomb's friction law (12), the discretization is as follows:

$$-u_{t,i+1} \in N_{C(\mu r_{n,i+1})}(r_{t,i+1}). \quad (23)$$

4.3 Problem formulation

Using the equations (3) and (4), the discretization of the equation of motion and of the contact law can be summarized in the following system :

$$\begin{cases} \mathbb{W} \mathbf{r}_{i+1} - \mathbf{u}_{i+1} = -\mathbf{u}_{free} \\ law_\alpha[\mathbf{u}_{\alpha,i+1}, \mathbf{r}_{\alpha,i+1}] = .true., \quad \alpha = 1, \dots, n_c \end{cases} \quad (24)$$

where $\mathbb{W} (= \mathbb{H}^* \mathbb{M}^{-1} \mathbb{H})$ is the Delassus operator, which models the local behavior of the solids at the contact points. The right-hand-side of the first equation in (24) represents the free relative velocity calculated by taking into account the internal and external forces $\mathbf{F}(t)$, only. The second equation in (24) requires that the frictional contact law law_α must be satisfied by each component of the couple $(\mathbf{u}, \mathbf{r})_\alpha$.

5 Various formulations of the 3D frictional contact problem

5.1 Linear Complementarity Problem (LCP) formulation

The LCP is a widespread in Mathematical Programming theory. A usual definition of this problem can be formulated as follows:

Problem 1 (Linear Complementarity Problem (LCP)). *Given $\mathbb{M} \in \mathbb{R}^{n \times n}$ and $\mathbf{q} \in \mathbb{R}^n$, find a vector $\mathbf{z} \in \mathbb{R}^n$ such that*

$$\mathbf{0} \leq \mathbf{z} \perp \mathbb{M}\mathbf{z} + \mathbf{q} \geq \mathbf{0} \quad (25)$$

The inequalities have to be understood componentwise and the relation $\mathbf{x} \perp \mathbf{y}$ means $\mathbf{x}^T \mathbf{y} = 0$.

5.1.1 The frictionless case

For the frictionless contact problem, the relation between (24) and (25) is direct: \mathbb{M} is equal to the Delassus operator \mathbb{W} and \mathbf{q} to \mathbf{u}_{free} , and the vector \mathbf{z} is the vector of reaction and impulses \mathbf{r}_{i+1} .

5.1.2 The frictional case

Contrary to the 2D frictional contact problem, the 3D case can not be casted directly into an LCP, mainly due to the non linear feature of the section of the friction cone, $C(\mu r_n)$. To overcome this difficulty, some approximations have been proposed which consist in a facetization of $C(\mu r_n)$. The following presentation is partly inspired from [15] where a very clear and concise presentation can be found.

Outer approximation by a polytope. Following the work of [21, 22], the friction disk $C(\mu r_n)$ can be approximated by :

$$C_{outer}(\mu r_n) = \bigcap_{i=1}^{\nu} C_i(\mu r_n) \quad \text{with } C_i(\mu r_n) = \{ \lambda_t \sigma_i(\lambda_t) = \mu r_n - \mathbf{c}_i^T \lambda_t \geq 0 \} \quad (26)$$

The functions $\sigma_i(\lambda_t)$ are the friction saturations with respect to the cone $C_i(\mu r_n)$ generated by an outward unit vector \mathbf{c}_i (e.g. Fig. 1a)). We now assume that the contact law (13) is of the form

$$-\mathbf{u}_t \in N_{C_{outer}(\mu r_n)}(\mathbf{r}_t) \quad (27)$$

From [37], the normal cone to $C_{outer}(\mu r_n)$ is given by :

$$N_{C_{outer}(\mu r_n)}(\mathbf{r}_t) = \sum_{i=1}^{\nu} N_{C_i(\mu r_n)}(\mathbf{r}_t) \quad (28)$$

and the inclusion can be stated in terms of the following complementarity problem :

$$-\mathbf{u}_t \in \sum_{i=1}^{\nu} -\kappa_i \partial \sigma_i(\lambda_t), \quad 0 \leq \sigma_i(\lambda_t) \perp \kappa_i \geq 0 \quad (29)$$

Since $\sigma_i(\lambda_t)$ is linear with respect to λ_t , we obtain the following LCP :

$$-\mathbf{u}_t \in \sum_{i=1}^{\nu} -\kappa_i \mathbf{c}_i, \quad 0 \leq \sigma_i(\lambda_t) \perp \kappa_i \geq 0 \quad (30)$$

Grouping the equations (24), (22) and (30), the one step nonsmooth problem that we have to solve reduces to a LCP.

Inner approximation by a polytope. The principle of an inner approximation is exposed for different purposes in [5] and [42]. The idea is to approach the friction disk by a interior polygon with ν edges. (e.g. Fig.1b)):

$$C_{inner}(\mu r_n) = \{\lambda_t = \mathbb{D}\beta, \beta \geq 0, \mu r_n \geq e_T \beta\} \quad (31)$$

where $\mathbf{e} = [1, \dots, 1]^T \in \mathbb{R}^\nu$, the columns of the matrix \mathbb{D} are the directions vector \mathbf{d}_j which represent the vertices of the polygon. For the sake of simplicity, we assume that for every i there is j such that $\mathbf{d}_i = -\mathbf{d}_j$. Following the same process as in the previous case and rearranging the equations, we obtain the following LCP :

$$\begin{cases} \mathbf{r}_t = \mathbb{D}\beta \\ 0 \leq \beta \perp \lambda \mathbf{e} + \mathbb{D}^T v_t \geq 0 \\ 0 \leq \lambda \perp \lambda \perp \mu r_n - e_T \beta \geq 0 \end{cases} \quad (32)$$

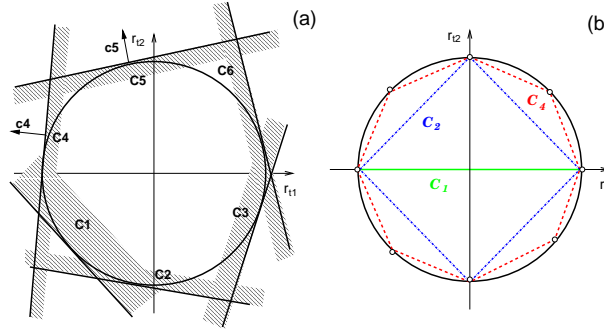


Figure 1: Approximation of the base of the Coulomb cone by an outer approximation (a) and by an interior 2ν -gon (b)

Thus using a projection operator with can express the frictional contact problem as a LCP($\tilde{\mathbf{q}}, \tilde{\mathbb{M}}$) with $\tilde{\mathbb{M}} \in \mathbb{R}^{m \times m}$, $\tilde{\mathbf{q}} \in \mathbb{R}^m$ and $m = n(2 + \nu)$. Through this formulation allows one to deal with frictional problems, it increases drastically the number of unknowns.

5.2 Mixed Complementarity problem (MCP)

When only box constraints are encountered, we obtain the so-called Mixed Complementarity problem given by :

Problem 2 (Mixed Complementarity Problem (MCP)). Given a mapping $F : \mathbb{R}^n \mapsto \mathbb{R}^n$, bounds $\mathbf{b}_l, \mathbf{b}_u \in \mathbb{R}^n \cup \{-\infty, +\infty\}$, find a vector $\mathbf{z} \in \mathbb{R}^n$ and vectors $\mathbf{v}, \mathbf{w} \in \mathbb{R}^n$ such that

$$\begin{cases} F(\mathbf{z}) = \mathbf{w} - \mathbf{v} \\ \mathbf{0} \leq (\mathbf{z} - \mathbf{b}_l) \perp \mathbf{w} \geq \mathbf{0} \\ \mathbf{0} \leq \mathbf{v} \perp (\mathbf{b}_u - \mathbf{z}) \geq \mathbf{0} \end{cases} \quad (33)$$

6 Iterative numerical solution methods

As Glocker mentioned in [15], a good solver has to deal correctly with two difficulties apart from the real-time constraint. The first one is the redundancy and the linear dependency of the

constraints which is usual in large systems of rigid bodies. This problem can be also viewed as the lack of definite positiveness of the Delassus operator. The second difficulty is that the structure of the discretized problem may change drastically at each time-step. Fortunately, the second difficulty is correctly grasped by the inherent structure of the presented time-stepping.

In order to solve the various problems formulated in the previous section, two choices are available: direct (pivoting) or iterative (splitting) methods [10]. The advantages of the first ones (the results are expected in a finite number of operations) give to such methods the preponderance for problems of small size, where they are probably as good as any other kind of methods. Such types of methods are however very sensitive to the well-posedness of the formulation (definite positiveness, independence of the constraints). For larger systems their efficiencies can be turned off for two reasons: *Data Storage* and *round-off errors*. The first point is strongly related to the computer architecture and the second one can lead to incorrect pivots. Nevertheless, to do a comparison with a direct pivoting method, we have chosen the Lemke's algorithm [10]. Iterative algorithms can be seen as an alternative to pivoting methods when the size of problem increases. Contrary to previous schemes, they are not finite but we can expect that iterates converges quickly to a solution. The fact that we have a "not so bad" first guess for the iterative solver keeping the values of the previous step is also an advantage. But one of the biggest advantage of iterative schemes lies in the fact that we can approach very quickly a rough estimate of the solution, instead of waiting for the complete termination of a direct algorithm. This point is crucial for the real-time applications where a rough approximation in time is better than nothing.

6.1 A General splitting scheme

Many iterative methods for solving system (24), reformulated as the LCP(\mathbf{q}, \mathbb{M}) (25), can be described by a matrix splitting (see [10] for a detailed version). The principle is to decompose the matrix \mathbb{M} as the sum of two matrices \mathbb{B} and \mathbb{C} which define the splitting. Thus the LCP(\mathbf{q}, \mathbb{M}) is transformed into a fixed-point problem. For an arbitrary vector \mathbf{z} we consider the LCP(\mathbf{q}^z, \mathbb{B}) with

$$\mathbf{q}^z = \mathbf{q} + \mathbb{C}\mathbf{z}.$$

If the vector \mathbf{z} is obtained as a solution of the LCP(\mathbf{q}^z, \mathbb{B}), it is also a solution of the LCP(\mathbf{q}, \mathbb{M}) [10].

The three steps of the iterative method to solve the LCP(\mathbf{q}, \mathbb{M}) are the following:

General splitting scheme:

Step 0: Initialization with \mathbf{z}^0 non negative.

Step 1: Iteration loop \mathbf{z}^{k+1} solution of the LCP(\mathbf{q}^k, \mathbb{B}) with $\mathbf{q}^k = \mathbf{q} + \mathbb{C}\mathbf{z}^k$.

Step 2: If error criteria is satisfied, \mathbf{z}^{k+1} is solution else increment k and return to **Step 1**.

Note that the quality of the solution is governed by the error criteria. A large number of iterations leads (a fortiori) to a good solution to the detriment of the CPU time. So a good compromise must be found between acceptable solutions and CPU time, especially in the context of real-time simulations. When the problem (25) is only a unilateral problem, as a splitting of \mathbb{M} we can take

$$\mathbb{B} = \mathbb{L} + \omega^{-1}\mathbb{D}$$

where \mathbb{L} and \mathbb{D} are respectively the strictly lower triangular and diagonal part of \mathbb{M} and where $\omega \in (0, 2)$ is an arbitrary relaxation parameter. In this case we obtain a *Projected Successive*

Over Relaxation scheme (PSOR) where the iterate \mathbf{z}^{k+1} is given by

$$z_i^{k+1} = \max(0, z_i^k - \omega M_{ii}^{-1}(q_i + \sum_{j<i} M_{ij} z_j^k + 1 + \sum_{j\geq i} M_{ij} z_j^k)), \quad i = 1, \dots, n. \quad (34)$$

The word *Projected* refers to the projection on the non negative orthant related to the unilateral constraint. When $\omega = 1$ the PSOR method is equal to the projected or Non Smooth Gauss Seidel algorithm. Thus the input of the algorithm are the same that for system (25).

6.2 Block Non Smooth Gauss-Seidel (NSGS) for frictional problems

We present in this section a specification of the general splitting method dedicated to the frictional-contact problem, the so-called *Block Non Smooth Gauss-Seidel algorithm* (NSGS) exposed in [19]. This solver has been proved to be very robust and efficient on a large collection of heterogeneous problems, see [4, 2, 19, 31, 32, 36, 40, 39]. This specification is based on two remarks. This first one is that the Delassus operator is usually Block structured in multibody dynamics. Therefore, we choose a splitting taking advantage of this fact. The matrix \mathbb{D} is composed to the block on the diagonal of \mathbb{M} and the matrix \mathbb{L} to the lower triangular block matrix. This algorithm can be stated using the notation of system (24) as

$$\begin{cases} \mathbf{u}_\alpha^{k+1} - \mathbb{W}_{\alpha\alpha} \mathbf{r}_\alpha^{k+1} = \mathbf{u}_{\alpha,free} + \sum_{\beta<\alpha} \mathbb{W}_{\alpha\beta} \mathbf{r}_\beta^{k+1} + \sum_{\beta>\alpha} \mathbb{W}_{\alpha\beta} \mathbf{r}_\beta^k \\ law_\alpha(\mathbf{u}_\alpha^{k+1}, \mathbf{r}_\alpha^{k+1}) = .true. \end{cases} \quad (35)$$

where $\mathbb{W}_{\alpha\beta}$ represents a block of the Delassus operator, and the index k refers to the algorithm iterations. The time index is omitted to make pleasant reading.

The subproblem $law_\alpha(\mathbf{u}_\alpha^{k+1}, \mathbf{r}_\alpha^{k+1}) = .true.$ must be solved by sequentially solving a finite number. The second remark for the specification OH the general splitting method is that the subproblem corresponds to the problem of frictionless/frictional contact for a single contactor α . In the frictionless case, the sub-LCP can be solved analytically. In the frictional case, the local resolution consists in finding the couple $(\mathbf{u}_\alpha^{k+1}, \mathbf{r}_\alpha^{k+1})$, which satisfies the relations of system (35). We denote \mathbf{b}_α^{k+1} the right-hand side of the first equation in (35). In 3D the Delassus Operator \mathbb{W} is a concatenation of n_c^2 matrices $\in \mathbb{R}^{3 \times 3}$ where the number of non null block matrices $\mathbb{W}_{\alpha,\beta}$ is related to the number of adjacent contacts to the contact α . The local frictional contact problem is described by the following scheme:

Explicit local resolution for the subproblem:

- Step 1:** If $b_{\alpha,n}^{k+1} < 0$ then there is no contact and we stop with $\mathbf{r}_\alpha = \mathbf{0}$
- Step 2:** The contact is active and we compute $\mathbf{r}_\alpha = (\mathbb{W}_{\alpha,\alpha})^{-1} \mathbf{b}_\alpha^{k+1}$
- Step 3:** If $\|\mathbf{r}_{\alpha,T}\| \leq \mu r_{\alpha,n}$, the contact is sticking (the tangential component is inside the friction cone) and we stop with no correction on the local impulse.
- Step 4:** The tangential component is outside the friction cone. We proceed to a correction of the local impulse as $\mathbf{r}_{\alpha,T} = p \mathbf{r}_{\alpha,T}$ with $p = \mu r_{\alpha,n} / \|\mathbf{r}_{\alpha,T}\|$

For spherical bodies the block $\mathbb{W}_{\alpha,\alpha}$ is diagonal and so easily invertible. Thus the local resolution can be written explicitly. In the case of contact, we proceed to a prediction of the tangential component of the local impulse. If the tangential component remains in the section of the cone (e.g. Fig. 2a) we keep the value of $\mathbf{r}_{\alpha,T}$ and the status of contact is *sticking*. In the

contrary case (e.g. Fig. 2b) we proceed to a correction of $\mathbf{r}_{\alpha,T}$, which corresponds to a radial projection of $\mathbf{r}_{\alpha,T}$ on the section of the cone. So the status is *sliding*.

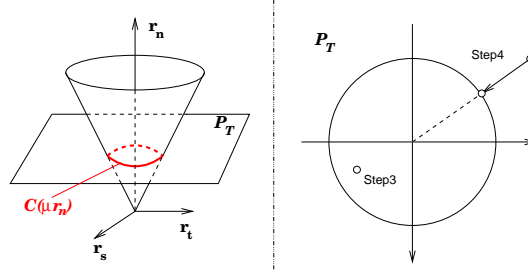


Figure 2: Friction cone and correction of the tangential component of the local impulse.

Note that for more general shapes $\mathbb{W}_{\alpha,\alpha}$ is no longer diagonal. The algorithm requires the inversion of all block diagonal matrices before the iterative process. This inversion is very important for the stability of the solution. The block diagonal matrix contains the relation between normal and tangential components. If we use a diagonalisation of it as performed in [39], we observe erratic behavior. With the inverse of the full matrix, the stability is ensured.

6.3 Conjugate Projected Gradient

It is also possible to reformulate the system (24) as an optimization problem using the contact impulses \mathbf{r} as the primal variable. When the Coulomb law is used the problem is no more an optimization problem but an "quasi"-optimization one due to the relation between the friction threshold and the normal component of the contact force. So problem (24) can be expressed as

$$\mathbf{r} \in \operatorname{argmin}_{\tilde{\mathbf{r}} \in \mathcal{C}(\mu r_n)} \frac{1}{2} \tilde{\mathbf{r}} \cdot \mathbb{W} \tilde{\mathbf{r}} - \mathbf{b} \cdot \tilde{\mathbf{r}}. \quad (36)$$

To solve (36) we used a conjugate projected gradient algorithm introduced by [34]. The authors proposed a more general and synthetic formulation than usual algorithms. Their improvement in regards of general conjugate gradient scheme is to conjugate the previous descent direction with the current gradient after projecting them on the set of active constraints. Extension for the three-dimensional case have been proposed [35] but was handicapped by the non polyhedral feature of the constraint set. We present here the outline of the algorithm and refer to [34, 35] for a fully detailed version.

If we denote $\mathbf{g}^k = \mathbf{b} - \mathbb{W} \mathbf{r}^k$ the residue and \mathbf{p}^k the descent direction, the *Conjugate Projected Gradient* algorithm (CPG) can be described by the following scheme:

The projection performed during the correction of step 2 is the projection on the Coulomb cone as the one performed on Fig. 2. The gradient projections of step 4 are respectively performed on the tangent cone T_C and on the subspace (of active constraints) to which \mathbf{w}^k belongs, after projection of \mathbf{u}^k , noted $A(\mathbf{w}^k)$.

7 Mixed iterative/pivoting Method : The PATH solver

The PATH solver [12, 13] is an implementation of the damped Newton method which makes use of the mixed complementarity formulation (MCP). The solver needs the definition of the

Conjugate Projected Gradient algorithm:

Step 0: Initialization : with a initial non negative vector \mathbf{r}^0 we compute \mathbf{g}^0 and $\mathbf{p}^0 = \mathbf{g}^0$

Step 1: Prediction of the local impulse : $\mathbf{r}^{k+\frac{1}{2}} = \mathbf{r}^k + \alpha^{k+1}\mathbf{p}^k$ with $\alpha^{k+1} = \frac{\mathbf{u}^k \cdot \mathbf{p}^k}{\mathbf{p}^k \cdot \mathbb{W}\mathbf{p}^k}$

Step 2: Iterate correction : $\mathbf{r}^{k+1} = \text{proj}_{\mathcal{C}}(\mathbf{r}^{k+\frac{1}{2}})$

Step 3: Residue computation : $\mathbf{u}^{k+1} = \mathbf{b} - \mathbb{W}\mathbf{r}^{k+1}$. If error criteria is satisfied stop.

Step 4: Gradient projection : $\mathbf{w}^{k+1} = \text{proj}(\mathbf{u}^{k+1}; T_{\mathcal{C}}(\mathbf{r}^{k+1}))$ and $\mathbf{z}^{k+1} = \text{proj}(\mathbf{p}^k; A(\mathbf{w}^{k+1}))$

Step 4: Gradient conjugaison : $\mathbf{p}^{k+1} = \mathbf{w}^{k+1} + \beta^{k+1}\mathbf{z}^{k+1}$ with $\beta^{k+1} = \frac{\mathbf{w}^{k+1} \cdot \mathbb{W}\mathbf{p}^k}{\mathbf{p}^k \cdot \mathbb{W}\mathbf{p}^k}$

mapping F , assumed to be sufficiently smooth to define the Jacobian $Jac(F)$ of the mapping in the classical sense.

8 Simulation results

8.1 Conservative scheme

As said in Sec. 4, the θ -method is a scheme identical to the Euler's one when $\theta = 1$. In this case the scheme is dissipative and the total energy balance decreases during the simulation. On the contrary when $\theta = \frac{1}{2}$, the time integrator scheme is conservative and the loss of energy depends only of the contact/impact description: This is an important point in virtual reality. To illustrate this phenomena, we have simulated an elastic bouncing column composed of eight spheres. The friction is set to 0 to avoid friction effects. The normal restitution coefficient is equal to 1.

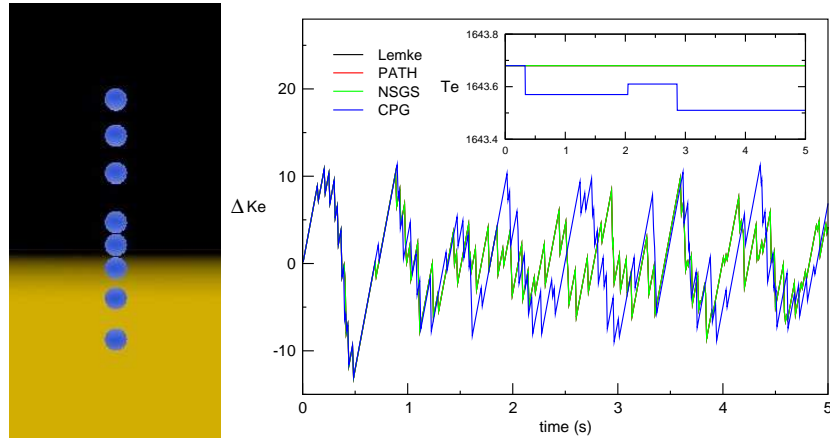


Figure 3: Elastic Bouncing column : the parameter of the θ -method is equal to $\frac{1}{2}$ and the restitution coefficient is equal to 1.

We compute two quantities: ΔKe which represents the variation of kinetic energy during on time step and Te which is the total energy in the system (potential plus kinetic). The simulation was performed using the solvers exposed previously and the evolutions of ΔKe and Te are plotted on Fig. 3. The first positive point is that the total energy is constant during the simulation for the Lemke's , PATH and NSGS method. Moreover the variations of ΔKe obtained with the previous solvers are rigorously identical. Indeed a different behavior is obtained with the CPG algorithm. The variation of ΔKe does not match the previous curves and Te is not constant on the time interval but constant on four subintervals. This observation can be explained by

error criteria used with the CPG method. In addition to convergence test performed at the step 3 of the algorithm, a test is performed before the computation of α (step 1). In our version of the algorithm, when the product $\mathbf{p}^k \cdot \mathbb{W}\mathbf{p}^k$ vanishes, we stop the algorithm and use the latest value obtained during iteration to continue computation. This modification leads to obtain some solution which do not respect exactly the energy balance. Nevertheless the lost energy quantity is quite small with regard to the total energy value. In spite of the phenomena, we can say that it is an acceptable solution.

8.2 The pyramidal cone weakness

To face three-dimensional frictional contact problems, usually the Coulomb friction cone is approached by a pyramidal one. We illustrate some weaknesses of this approach on the following example. Let's consider a spherical ball lying on a horizontal plan. Gravity is considered and we denote g its norm. We apply to the ball a cycling external force defined as

$$\mathbf{F}_c(t) = \begin{cases} \mu mg(\cos \frac{\pi}{3} \mathbf{e}_x + \sin \frac{\pi}{3} \mathbf{e}_y) & \forall t \in [15k, 5 + 15k[\\ -\mu mg \mathbf{e}_x & \forall t \in [5 + 15k, 10 + 15k[\\ \mu mg(\cos \frac{\pi}{3} \mathbf{e}_x + -\sin \frac{\pi}{3} \mathbf{e}_y) & \forall t \in [10 + 15k, 15(k + 1)[\end{cases}, \quad k \in \mathbf{N}. \quad (37)$$

The norm of $\mathbf{F}_c(t)$ is chosen to active the sliding motion of the ball and to coincide the initial and the final point of a cycle coincide. Thus during simulations, the trajectory of the ball must match with an equilateral triangle. Figure 4a) represents the trajectories obtained with NSGS without approximation (*w.a.*) and with a C_2 approximation and Figure 4b) depicts the trajectories obtained with the Lemke's algorithm with the C_i approximations ($i \in \{2, 3, 4, 6, 8\}$).

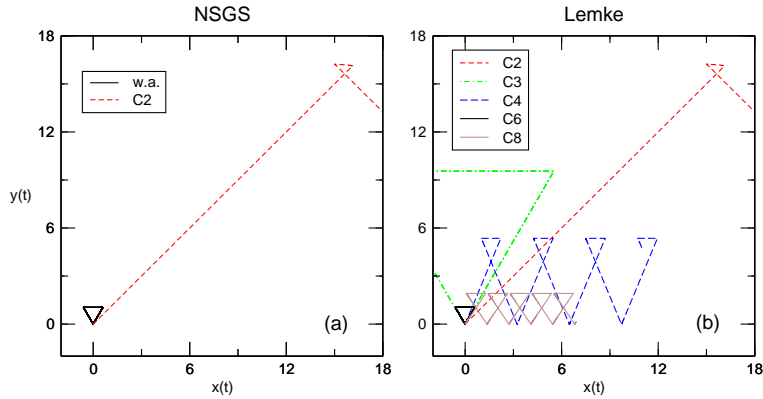


Figure 4: Ball trajectory under cycling loading using NSGS (a) and Lemke (b) algorithms

The computation without this approximation matches with the analytical solution. On the contrary computations using approximation (with Lemke as well as NSGS) can lead to unrealistic behavior. To approach the solution we must use a high order approximation introducing a higher number of unknowns. So a first advantage is given to the dedicated methods, such as the NSGS and CPG, which can deal with no approximation of the friction cone and preserve the size of the system.

8.3 Compact assemblies

The Computer Graphics community has proposed some approaches to simulate large stacking and piles of rigid bodies (e.g. [16, 41]) but without respect of the real-time constraint. With-

out this hard constraint, the three dimensional simulations of Saussine et al [39] seems however to be more powerful.

With the respect of the real-time constraint, the number of simulated bodies is not so large and our aim is clearly to perform *real-time simulation of dynamical multibody systems*. To illustrate our first results we have chosen two samples of dense assemblies: sphere settling (e.g. Fig 5a)) and virtual masonry (e.g. Fig 5b)).

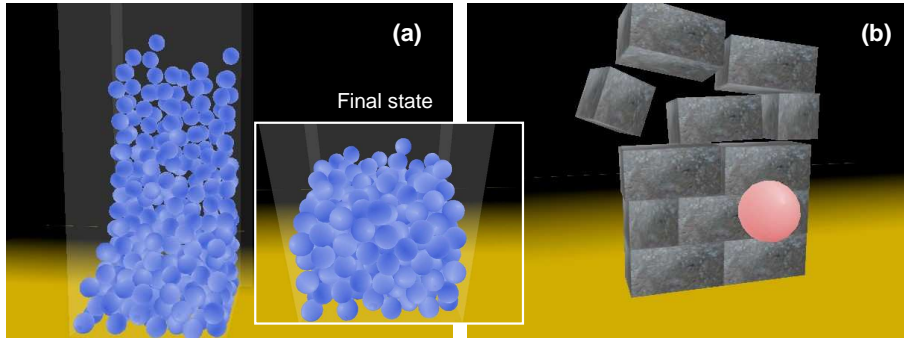


Figure 5:

Sphere settling We define the following parameters: the time-step value h , g_{max} as the maximal inter penetration between contactors in the sample. The rule is to find h such as we preserve a smaller value of g_{max} to ensure the quality of the simulation and the real-time constraint. We denote S_p the ratio between the simulated-time and the elapsed CPU time. The real-time constraint will be preserved if $S_p \geq 1$. We performed settling in a box with a frictional contact interaction law and using different numbers of spheres : 80, 160 and 320. Simulation results are shown in the Tab. 1.

n_b	n_c	h	S_p	$g_{max}(\%)$
80	271	0.02	1.24	0.3
80	267	0.04	2.28	1.2
160	587	0.02	0.95	0.5
160	584	0.04	1.50	1.8
320	1218	0.02	0.50	0.6
320	1275	0.04	0.75	2.2

Table 1: Results of simulation of sphere settlings

The simulations of samples composed of 80 and 160 spheres respect the real-time constraint and keep a good quality (less than 2% of violation). For the bigger one (320 spheres), it is difficult to preserve both the time constraint and the quality of solution. Nevertheless the value of the speed-up (0.75) is not so small and some numerical optimization should enable to obtain the respect of the time-constraint. Note that for the frictionless packing, the real-time constraint is reached for the larger sample: the time needed by the solver is smaller due to the smaller number of unknowns.

The difficulty in this kind of simulation is the large variation in the contact number. It increases

quickly to reach a stabilized value (e.g. Fig. 6b)). The large number of status modifications does not help the frictional contact solver to reach a solution. During the settling, the number of iterations N_{it} reaches the maximal value ($\in [0, 15]$) and during a stabilization phase ($t \in [15, 35]$) N_{it} has erratic variations from the minimal to the maximal value to keep a stabilized evolution below. The fact that iterative methods can benefit from the solution of the previous time step to initialize the algorithm is one of the reasons of the quasi-smooth evolution. Moreover with an iterative method a good approximation of the solution is obtained quickly as show in Fig. 6a). For a sample with 600 contacts, an approximation of the solution with an error of 10% is obtained in 10 iterations only.

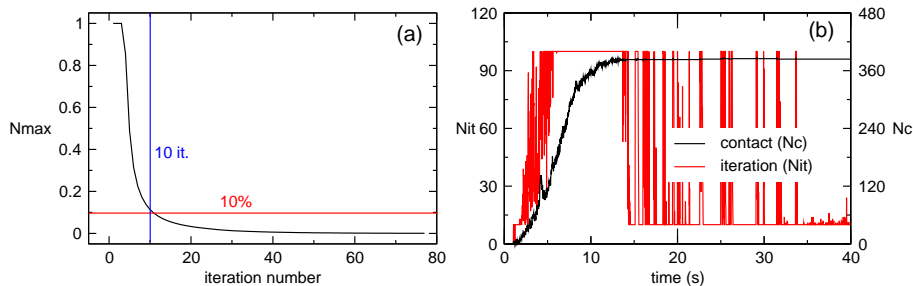


Figure 6: a) Evolution of the convergence criterion during the iterative process. b) Parallel between the evolution of iterations and the number of contacts during a whole simulation process.

Virtual masonry Some difficulties are related to the numerical simulation of masonry structures. The first one is related to the location of the contact point and their number. When we consider two blocks in a contact face/face, four dependent contacts at least are considered. This strategy, which preserves the time taken by the detection algorithm, handicap direct method as Lemke.

The second one concerns the introduction of friction. When the problem is formulated as an LCP problem, the matrix of the LCP is no longer symmetric. This appear as a problem for Lemke as well as the PATH solver. It may be related to the observation of Klarbring on the class of matrix unsolvable by LCP solver [21].

Iterative solvers appear here to be the more efficient ones to face this kind of sample. Note that in the local resolution the inverse of the full matrix must be considered to ensure the stability of the structure.

9 Concluding discussion

In this kind of simulations the matrix of our system is only positive semi-definite due to the numerous connections between bodies. Direct methods such as Lemke appear inefficient to solve such a LCP. On the contrary iterative methods seem to be able to overcome this indeterminacy and converge towards a solution among the several admissible ones. The clever MCP formulation of Glocker [15], or the particular treatment of degenerate QP in [14] may bring interesting solutions.

Acknowledgment

The post doctoral fellowship of the first author has been supported by the INRIA for a collaboration between the SIAMES and BIPOP projects. The second author wants to acknowledge

Michael Ferris for the PATH solver and the valuable discussions on algorithms. The authors thank Pr. Brogliato for his relevant remarks.

REFERENCES

- [1] M. Abadie. Dynamic simulation of rigid bodies: Modelling of frictional contact. In B. Brogliato, editor, *Impacts in Mechanical Systems: Analysis and Modelling*, volume 551 of *Lecture Notes in Physics (LNP)*, pages 61–144. Springer, 2000.
- [2] V. Acary. *Contribution to the mechanical and numerical modelling of masonry structures*. Mémoire de Thèse de Doctorat, Supervisor: Michel Jean, Ecole Supérieure de Mécanique de Marseille, Université d’Aix-Marseille II, 5 janvier 2001. (in french).
- [3] V. Acary and B. Brogliato. Concurrent multiple impacts modelling - case-study of a 3-ball chain. In K. J. Bathe, editor, *Second MIT conference on computational Fluid and Solid Mechanics*, pages 1842–1847. Elsevier, jun 2003.
- [4] V. Acary and M. Jean. Numerical modeling of three dimensional divided structures by the non smooth contact dynamics method: Application to masonry structure. In B.H.V. Topping, editor, *The Fifth international Conference on Computational Structures Technology 2000*, pages 211–222. Civil-Comp Press, 6-8 September 2000.
- [5] A. M. Al-Fahed, G. E. Stavroulakis, and P. D. Panagiotopoulos. Hard and soft fingered robot grippers. The linear complementarity approach. *Z. angew. Math. Mech.*, 71:257–265, 1991.
- [6] D. Baraff. Analytical methods for dynamic simulation of non-penetrating rigid bodies. In *Proceedings of SIGGRAPH ’89*, pages 223–232. ACM Press, 1989.
- [7] D. Baraff. Fast contact force computation for nonpenetrating rigid bodies. In *Proceedings of SIGGRAPH ’94*, pages 23–34. ACM Press, 1994.
- [8] B. Brogliato, AA. ten Dam, L. Paoli, F. Génot, and M. Abadie. Numerical simulation of finite dimensional multibody nonsmooth mechanical systems. *Appl. Mech. Rev.*, 55(2):107–149, 2002.
- [9] M. Buck and E. Schömer. Interactive rigid body manipulation with obstacle contacts. *J. Visu. Comput. Anim.*, 9(4):243–257, 1998.
- [10] R. W. Cottle, J. Pang, and R. E. Stone. *The linear complementarity problem*. Academic Press, Inc., Boston, MA, 1992.
- [11] P. A. Cundall. A computer model for simulating progressive large scale movements of blocky rock systems. In *Proceedings of the symposium of the international society of rock mechanics*, volume 1, pages 132–150, 1971.
- [12] S. P. Dirkse and M. C. Ferris. The path solver: A non-monotone stabilization scheme for mixed complementarity problems. *Optimization Methods and Software*, 5:123–156, 1995.
- [13] M. C. Ferris and T. S. Munson. Interfaces to path 3.0: Design, implementation and usage. *Comput. Optim. Appl.*, 12(1-3):207–227, 1999.

- [14] R. Fletcher. Resolving degeneracy in quadratic programming. *Annals of Operations Research*, 46–47(1–4):307–334, 1993.
- [15] C. Glocker. Formulation of spatial contact situations in rigid multibody systems. *Comput. Methods Appl. Mech. Engrg.*, 177:199–214, 1999.
- [16] E. Guendelman, R. Bridson, and R. Fedkiw. Nonconvex rigid bodies with stacking. *ACM Trans. Graph.*, 22(3):871–878, 2003.
- [17] J. K. Hahn. Realistic animation of rigid bodies. In *Proceedings of SIGGRAPH '88*, pages 299–308. ACM Press, 1988.
- [18] S. Hasegawa, F. Nobuaki, Y. Koike, and M. Sato. Real-time body simulation based on volumetric penalty method. In *Proceedings of HAPTICS '03*, pages 326–332, 2003.
- [19] M. Jean. The non smooth contact dynamics method. *Compt. Methods Appl. Math. Engrg.*, 177:235–257, 1999.
- [20] M. Jean and J. J. Moreau. Unilaterality and dry friction in the dynamics of rigid bodies collection. In A. Curnier, editor, *Contact Mechanics International Symposium*, pages 31–48. Presses Polytechniques et Universitaires Romanes, 1992.
- [21] A. Klarbring. A mathematical programming approach to three-dimensional contact problem with friction. *Compt. Methods Appl. Math. Engrg.*, 58:175–200, 1986.
- [22] A. Klarbring and G. Björkman. A mathematical programming approach to contact problems with friction and varying contact surface. *Computers & Structures*, 30(5):1185–1198, 1988.
- [23] J. E. Loyd, J. S. Beis, D. K. Pai, and D. G. Lowe. Programming contact tasks using a reality-based virtual environment integrated with vision. *IEEE Transaction on Robotics and Automation*, 15(3):423–434, June 1999.
- [24] M. Mabrouk. A unified variational model for the dynamics of perfect unilateral constraints. *Eur. J. Mecha. A Solids*, 17(5):819–842, 1998.
- [25] V. J. Milenkovic. Position-based physics: Simulating the motion of many highly interacting spheres and polyhedra. In *Proceedings of SIGGRAPH '96*, pages 129–136. ACM Press, 1996.
- [26] V. J. Milenkovic and H. Schmidl. Optimization-based animation. In *SIGGRAPH '01: Proceedings of the 28rd annual conference on Computer graphics and interactive techniques*, pages 37–46. ACM Press, 2001.
- [27] B. Mirtich and J. Canny. Impulse-based simulation of rigid bodies. In *Proceedings of SI3D '95*, pages 181–188. ACM Press, 1995.
- [28] M. D. P. Monteiro Marques. *Differential Inclusions in Nonsmooth Mechanical Problems: Shocks and Dry Friction*, volume 9 of *Progress in Nonlinear Differential Equations and Their Applications*. Birkhauser Verlag, Basel, Boston, Berlin, 1993.

- [29] M. Moore and J. Wilhems. Collision detection and response for computer animation. In *Proceedings of SIGGRAPH '88*, pages 289–298. ACM Press, 1988.
- [30] J. J. Moreau. Unilateral contact and dry friction in finite freedom dynamics. In J.J. Moreau and eds. P.-D. Panagiotopoulos, editors, *Non Smooth Mechanics and Applications, CISM Courses and Lectures*, volume 302 (Springer-Verlag, Wien, New York), pages 1–82, 1988.
- [31] J. J. Moreau. Some numerical methods in multibody dynamics: application to granular materials. *Eur. J. Mech. A Solids*, 13(4-suppl.):93–114, 1994.
- [32] J. J. Moreau. Numerical aspect of sweeping process. *Compt. Methods Appl. Math. Engrg.*, 177:329–349, 1999.
- [33] F. Pfeiffer and C Glocker, editors. *Multibody dynamics with unilateral contacts*. Non-linear Dynamicss. John Wiley and Sons, 1996.
- [34] M. Renouf and P. Alart. Conjugate gradient type algorithms for frictional multicontact problems: applications to granular materials. *Comp. Meth. Appl. Mech. Engrg.*, 194(18-20):2019–2041, 2004.
- [35] M. Renouf and P. Alart. Gradient type algorithms for 2d/3d frictionless/frictional multi-contact problems. In K. Majava P. Neittaanmaki, T. Rossi, O.Pironneau (eds.) R. Owen, and M. Mikkola (assoc. eds.), editors, *ECCOMAS 2004*, Jyvaskyla, 24–28 July 2004.
- [36] M. Renouf, F. Dubois, and P. Alart. A parallel version of the Non Smooth Contact Dynamics algorithm applied to the simulation of granular media. *J. Comput. Appl. Math.*, 168:375–38, 2004.
- [37] R.T. Rockafellar. *Convex Analysis*. Princeton University Press, 1970.
- [38] J. Sauer and E. Schömer. A constraint-based approach to rigid body dynamics for virtual reality applications. In *Proceedings of VRST '98*, pages 153–161. ACM Press, 1998.
- [39] G. Saussine, C. Cholet, P.E. Gautier, F. Dubois, C. Bohatier, and J. J Moreau. Modelling ballast under cyclic loading using discrete element method. In *Proceedings of International Conference on Cyclic Behaviour of Soils and Liquefaction Phenomena*. Balkema, April 2004.
- [40] G. Saussine, F. Dubois, C. Bohatier, C. Cholet, P.E. Gautier, and J.J. Moreau. Modelling ballast behaviour under dynamic loading, part 1: a 2d polygonal discrete element method approach. *to appear in Computer methods in applied mechanics and engineering*, 2004.
- [41] H. Schmidl and V.J. Milenkovic. A fast impulsive contact suite for rigid body simulation. *IEEE Transactions on Visualisation and Computer Graphics*, 10(2):189–197, March/April 2004.
- [42] D. E. Stewart and J. C. Trinkle. An implicit time-stepping scheme for rigid body dynamics with inelastic collisions and Coulomb friction. *Int. J. Num. Methods Engrg.*, 39:2673–2691, 1996.